

1 **Overview of the NOAA/ESRL Federated Aerosol Network**

2

3 Elisabeth Andrews<sup>1</sup>, Patrick J. Sheridan<sup>2</sup>, John A. Ogren<sup>2</sup>, Derek Hageman<sup>1</sup>, Anne Jefferson<sup>1</sup>,  
4 Jim Wendell<sup>2</sup>, Andrés Alastuey<sup>3</sup>, Lucas Alados-Arboledas<sup>4</sup>, Michael Bergin<sup>5</sup>, Marina Ealo<sup>3</sup>, A.  
5 Gannet Hallar<sup>6,7</sup>, Andras Hoffer<sup>8</sup>, Ivo Kalapov<sup>9</sup>, Melita Keywood<sup>10</sup>, Jeongeun Kim<sup>11</sup>, Sang-Woo  
6 Kim<sup>12</sup>, Felicia Kolonjari<sup>13</sup>, Casper Labuschagne<sup>14</sup>, Neng-Huei Lin<sup>15</sup>, AnneMarie Macdonald<sup>13</sup>,  
7 Olga L. Mayol-Bracero<sup>16</sup>, Ian B. McCubbin<sup>7</sup>, Marco Pandolfi<sup>3</sup>, Fabienne Reisen<sup>10</sup>, Sangeeta  
8 Sharma<sup>13</sup>, James P. Sherman<sup>17</sup>, Mar Sorribas<sup>18</sup>, Junying Sun<sup>19</sup>

9

10 <sup>1</sup>Cooperative Institute for Research in Environmental Sciences (CIRES), University of Colorado,  
11 Boulder, CO USA

12

13 <sup>2</sup>Earth System Research Laboratory (ESRL), National Oceanic and Atmospheric Administration  
14 (NOAA), Boulder, CO USA

15

16 <sup>3</sup>Institute of Environmental Assessment and Water Research, Barcelona, Spain

17

18 <sup>4</sup>Andalusian Institute for Earth System Research, IISTA-CEAMA, University of Granada,  
19 Granada, Spain

20

21 <sup>5</sup>Department of Civil & Environmental Engineering, Duke University, Durham, NC, USA

22

23 <sup>6</sup>University of Utah, Department of Atmospheric Science, Salt Lake City, UT, USA

24

25 <sup>7</sup>Storm Peak Laboratory, Desert Research Institute, Steamboat Springs, CO, USA

26

27 <sup>8</sup>MTA-PE Air Chemistry Research Group, University of Pannonia, Veszprém, Hungary

28

29 <sup>9</sup>Institute for Nuclear Research and Nuclear Energy, Basic Environmental Observatory

30 Moussala, Sofia, Bulgaria

31

32 <sup>10</sup>CSIRO Oceans and Atmosphere, Aspendale, Australia

33

34 <sup>11</sup>Environmental Meteorology Research Division, National Institute of Meteorological Sciences

35 (NIMS), Seogwipo-si, Jeju-do, R. Korea

36

37 <sup>12</sup>School of Earth and Environmental Sciences, Seoul National University, Seoul, Korea

38

39 <sup>13</sup>Environment and Climate Change Canada, Toronto, Ontario, Canada

40

41 <sup>14</sup>Climate Environmental Research Monitoring (CERM), South African Weather Service,

42 Stellenbosch, South Africa

43

44 <sup>15</sup>Department of Atmospheric Sciences, National Central University, Taoyuan, Taiwan

45

46 <sup>16</sup>Department of Environmental Science, University of Puerto Rico - Rio Piedras, San Juan,  
47 Puerto Rico, USA

48

49 <sup>17</sup>Department of Physics and Astronomy, Appalachian State University, Boone, NC, USA

50

51 <sup>18</sup>El Arenosillo Atmospheric Sounding Station, Atmospheric Research and Instrumentation  
52 Branch, National Institute for Aerospace Technology (INTA), Huelva, Spain

53

54 <sup>19</sup>State Key Laboratory of Severe Weather & Key Laboratory of Atmospheric Chemistry of  
55 CMA, Chinese Academy of Meteorological Sciences, Beijing, Peoples Republic of China

56

57 Corresponding author: Elisabeth Andrews,

58 Email: [betsy.andrews@noaa.gov](mailto:betsy.andrews@noaa.gov)

59 Address: NOAA/ESRL/GMD, 325 Broadway, Boulder, CO 80305, USA

60 Phone: 303-497-5171

61 <https://doi.org/10.1175/BAMS-D-17-0175.1>

62 *Final Form: 19 June 2018*

63 *Published Online: 15 February 2019*

64

65

66 **Overview of the NOAA/ESRL Federated Aerosol Network**

67

68 **Capsule**

69 The cooperative nature of NOAA's Federated Aerosol Network allows for collection of consistent  
70 datasets for evaluating regionally representative aerosol climatologies, trends, and radiative  
71 forcing at 30 sites around the world.

72

73 **Abstract**

74 In order to estimate global aerosol radiative forcing, measurements of aerosol optical properties  
75 are made by the NOAA Earth System Research Laboratory's Global Monitoring Division  
76 (ESRL/GMD) and their collaborators at 30 monitoring locations around the world. Many of the  
77 sites are located in regions influenced by specific aerosol types (e.g., Asian and Saharan desert  
78 dust, Asian pollution, biomass burning, etc.). This network of monitoring stations is a shared  
79 endeavor of NOAA and many collaborating organizations, including the World Meteorological  
80 Organization Global Atmosphere Watch (WMO/GAW) Program, the U.S. Department of Energy  
81 (DOE), several U.S. and foreign universities, and foreign science organizations. The result is a  
82 long-term, cooperative program making atmospheric measurements that are directly comparable  
83 with those from all the other network stations and with shared data access. The protocols and  
84 software developed to support the program facilitate participation in GAW's atmospheric  
85 observation strategy and the sites in the NOAA/ESRL network make up a substantial subset of  
86 the GAW aerosol observations. This paper describes the history of the NOAA/ESRL Federated  
87 Aerosol Network, details about measurements and operations and some recent findings from the  
88 network measurements.

89

90 **1. Introduction**

91 Climate change is one of the most important environmental, social, economic, and political  
92 issues facing the planet today. Aerosol particles may have either a warming or cooling effect at  
93 the top-of-atmosphere, depending both on properties of the aerosol and the underlying surface  
94 (IPCC, 2013). Atmospheric aerosol particles interact with solar radiation by absorbing and  
95 scattering light. The amount of scattering and absorption is a function of particle size,  
96 composition, and shape, as well as external variables like relative humidity (RH) and wavelength  
97 of incident light. The regional influence of aerosol particles on climate and weather tends to be  
98 stronger than their global average impact, due to their relatively short atmospheric lifetimes and  
99 inhomogeneity in sources and processing. Thus, to understand the global influence of aerosol  
100 particles, it is necessary to make long-term measurements at many regionally representative sites  
101 (e.g., Laj et al., 2009; Lund Myhre and Baltensperger, 2012). Short-term aerosol campaign  
102 measurements are typically designed to study specific processes and/or events, but long-term  
103 measurements are often needed to put such data into a broader context, e.g., to assess whether  
104 field campaign measurements represent that location and season, as well as for assessing trends  
105 and variability. Such long-term measurements can take the form of ground-based remote  
106 sensing, satellite-based remote sensing, and/or ground-based in-situ sites. While the focus here  
107 is on long-term, surface in-situ sites, it is important to recognize the synergy obtained when data  
108 from multiple independent platforms are combined (e.g., Ogren, 1995; Kahn et al., 2004, 2017;  
109 Anderson et al., 2005). For example, combining surface measurements with airborne or remote  
110 sensing platforms enables the connection of ground-based aerosol properties to vertically-  
111 resolved processes. While ground-based, in-situ measurements cannot represent the properties

112 of aerosols that are present in layers aloft, multi-year in-situ aerosol profiling measurements over  
113 two FAN sites in the US have shown that ground-based measurements of aerosol intensive  
114 properties such as single scattering albedo and scattering Ångström exponent can represent the  
115 climatology of those properties aloft under well-mixed conditions (Andrews et al., 2004;  
116 Sheridan et al., 2012).

117  
118 Numerous stations around the world make long-term in-situ measurements of regionally-  
119 representative aerosol optical properties. Originally, many of these sites were operated in  
120 isolation to address specific scientific goals with sampling and data protocols designed to meet  
121 those goals, making it difficult to utilize those data in wider studies and inter-comparisons  
122 (Kulmala et al., 2011). Several recent papers note the importance of consistent operational and  
123 data processing among sites in order to improve data quality control and access across locations  
124 (e.g., Kulmala et al., 2011; Wiedensohler et al., 2012). In contrast, some sites (e.g., the original  
125 NOAA Baseline Observatories, Bodhaine, 1983) were conceived as part of a network where  
126 similarities in instruments, protocols, and a common data archive resulted in complete intra-  
127 network consistency, although extra-network comparisons were limited by differences in data  
128 collection and/or treatment. Recognition of the need for consistent measurements drives the  
129 development of protocols for instruments and data treatment (e.g., WMO, 2016).

130  
131 This paper presents a description of the current NOAA Federated Aerosol Network (FAN),  
132 which evolved from the original NOAA baseline network. The two primary purposes of this  
133 paper are (1) to describe the current state of the FAN (including its member stations, the  
134 measurements common to most of the stations, and the sampling and measurement protocols)

135 and (2) to show examples of the science that is possible with a global network of this type. A  
136 number of earlier papers (e.g., Sheridan et al., 2001; Delene and Ogren, 2002; Sherman et al.,  
137 2015) touched on some aspects of this, utilizing small subsets of the network (1 to 4 stations)  
138 but, until now, there have been no papers describing the FAN in its entirety. . The paper begins  
139 with a brief history of the network, discusses the key measurements and measurement protocols  
140 made at network sites, describes the software for data acquisition and processing, and finally,  
141 presents an overview of scientific results from FAN measurements over the last 15 years.

142

## 143 **2. History of the NOAA Federated Aerosol Network**

144 The current network mission is to characterize the means, variability, and trends of climate-  
145 forcing properties of different types of aerosols, and to understand the factors that control these  
146 properties. In the 1970s, NOAA's Environmental Research Laboratories (ERL) Geophysical  
147 Monitoring for Climatic Change (GMCC) Program had the mission to detect changes (i.e.,  
148 trends, cycles) in the long-term global aerosol background values. To do so, GMCC conducted  
149 aerosol measurements at four baseline observatories. The original NOAA Baseline  
150 Observatories (Mauna Loa, Hawaii (MLO), the South Pole (SPO), American Samoa (SMO), and  
151 Barrow, Alaska (BRW)) appear along the left-hand side of Figure 1. These sites are remote from  
152 aerosol sources and typically represent clean background air, although, occasionally, they may  
153 be impacted by long range transport (e.g., Perry et al., 1999; Stone et al., 2007).

154

155 Since the initial founding of the baseline observatory network, the scientific understanding of the  
156 properties and impacts of atmospheric aerosols has improved considerably. In response to the  
157 finding that anthropogenic aerosols create a significant perturbation in the Earth's radiative

158 balance on regional scales (e.g., Bolin and Rodhe, 1976; Charlson et al., 1991), NOAA expanded  
159 its aerosol research program starting in 1992 to include four sites in North America: Bondville,  
160 Illinois (BND, collaboration with University of Illinois), Sable Island, Nova Scotia (WSA,  
161 collaboration with Environment and Climate Change Canada), Southern Great Plains (SGP,  
162 collaboration with US Department of Energy)) and Trinidad Head, California (THD). These site  
163 locations were chosen because they are at times impacted by anthropogenic aerosols and  
164 consequently address the need to better understand how human activity can influence the  
165 radiation balance. Although these sites were not as remote as the baseline observatories, they  
166 also were not close to major anthropogenic aerosol sources (e.g., Delene and Ogren, 2002) and  
167 typically provide measurements of regionally representative aerosol (e.g., Wang et al., 2018).  
168

169 ESRL/GMD's expertise in maintaining long-term measurements of aerosol optical properties  
170 (often at remote locales) did not go unnoticed. Colleagues from around the world contacted  
171 GMD for advice on station operations and instrument maintenance and the collaborative  
172 NOAA/ESRL Federated Aerosol Network was born. The concept for and, indeed, the name of  
173 the FAN, owes much to the development of the AERONET sunphotometer network in the mid-  
174 1990s (Holben et al., 1998). The definition of a federation is groups "*that have joined together*  
175 *for a common purpose*" (Collins, 2018). The descriptor 'federated' is appropriate as the result is  
176 a long-term, cooperative program with shared data access making atmospheric measurements  
177 that are directly comparable with all the other FAN stations. FAN collaborators contribute  
178 scientific interest, instruments, onsite technicians, long-term station costs, and operations support  
179 while NOAA contributes software for data acquisition and processing, as well as technical  
180 expertise. It is a true partnership where both sides are learning from each other. A major



181 advantage is that the NOAA software and protocols streamline data acquisition and processing  
182 (discussed below) so that more time can be spent on science. Since 2010, more than 50 papers  
183 using FAN network data have been published and multiple graduate theses have also been  
184 submitted. FAN support has also improved data submission to the World Data Center for  
185 Aerosols ([www.gaw-wdca.org](http://www.gaw-wdca.org)), both in terms of quantity of data submitted and quality and  
186 completeness of the submitted data sets.

187

188 Since 2004, 25 sites operated by numerous collaborators have joined FAN (prior to 2004 only six  
189 sites were in the network – NOAA’s four baseline observatories and 2 regional stations running  
190 NOAA instruments and supervised by NOAA scientists). Many of these new cooperative aerosol  
191 monitoring sites are situated in regions where significant aerosol forcing is anticipated, including  
192 locations in North America, Europe, and Asia. Figure 1 illustrates that, while there is reasonable  
193 global coverage, there are also some large spatial gaps (particularly in the southern hemisphere)  
194 due to finite funding resources and limited infrastructure as well as the lack of collaborators in  
195 those regions. NOAA has as major partners in these global and regional aerosol measurements  
196 the World Meteorological Organization Global Atmosphere Watch (WMO/GAW) Program, and  
197 several US and foreign universities and science agencies. Most of the collaborative stations are  
198 run under the auspices of the GAW network, thus FAN sites may be considered a substantial  
199 subset of the larger GAW surface in-situ aerosol monitoring network. (FAN data comprises  
200 approximately 1/3 of GAW’s surface aerosol optical property measurements and dominates  
201 contributions of optical properties to GAW outside of Europe). Table S1 provides more detail  
202 about the sites shown in Figure 1.

203

### 204 **3. Description of system**

205 The basic aerosol optical property measurements made at FAN sites are spectral aerosol light  
206 scattering (total and backwards hemisphere) and light absorption. These are the critical  
207 parameters for determining aerosol direct radiative forcing. Most of the sites also measure  
208 aerosol number concentration. Depending on the station, additional aerosol and gas-phase  
209 measurements may be available. Over the years, NOAA/GMD has developed protocols and  
210 instrument infrastructure in order to make measurements of known, high quality and has written  
211 software to enable consistent processing, editing, and archiving of the data. NOAA (2018a)  
212 provides details, design drawings and photos of the system components (inlet, instruments,  
213 auxiliary control units, pumpbox, etc.), but brief descriptions of the main components are  
214 provided below.

215

### 216 **3.1 Instruments**

217 Light scattering by atmospheric aerosols at the FAN stations is measured using integrating  
218 nephelometers (currently, either the TSI (model 3563, TSI Inc., St Paul, MN) or the Ecotech  
219 (Aurora 3000/4000, Ecotech, Melbourne, Australia) nephelometer). Both instruments measure  
220 total and hemispheric aerosol back-scattering coefficients at three visible wavelengths, enabling  
221 calculation of spectral aerosol properties and various proxies describing the angular distribution  
222 of light scattering (e.g., Andrews et al., 2006). Table S1 describes the scattering and absorption  
223 instruments at each site. Table S2 in the supplemental materials gives further details (e.g.,  
224 wavelengths) for the various instruments.

225

226 Aerosol light absorption is measured at FAN stations using a variety of filter-based absorption  
227 instruments. Currently, the primary light absorption instruments are the ESRL/GMD-developed

228 three-wavelength Continuous Light Absorption Photometer (CLAP, Ogren et al., 2017) and the  
229 single-wavelength Multi-Angle Absorption Photometer (MAAP, Thermo Fisher Scientific,  
230 Franklin, MA). Many sites are also operating 7-wavelength aethalometers (Magee Scientific,  
231 Berkeley, CA) to take advantage of that instrument's broad spectral range. Previously, FAN sites  
232 used single- and multi-wavelength Particle Soot Absorption Photometers (PSAP, Radiance  
233 Research Inc., Seattle, WA) and/or broadband aethalometers.

234

235 While the instruments across the FAN are not identical, laboratory studies suggest they make  
236 comparable measurements. Intercomparisons of TSI and Ecotech nephelometers show excellent  
237 reproducibility for total scattering although the differences are slightly larger for backscattering  
238 (Mueller et al., 2011b). Mueller et al. (2011a) find good agreement between PSAPs and MAAPs  
239 for a 2007 intercomparison study although less agreement existed for an earlier (2005) data set.  
240 Mueller et al (2011a) also identify a fairly wide range of variability in PSAPs, but show much of  
241 the variability was due to spot size variations and flow rate issues. The PSAPs and CLAPs in the  
242 FAN are corrected for spot size and operated at a consistent flow rate (face velocity of 0.8 m/s)  
243 to minimize these issues. Ogren et al. (2017) demonstrate excellent agreement between long-  
244 term measurements with PSAPs and CLAPs at multiple sites in the FAN. Sherman et al. (2015)  
245 present measurement uncertainties for scattering and absorption measurements as well as for  
246 calculated parameters **such as single scattering albedo and Ångström.**

247

248 Aerosol number concentration is another common measurement at FAN sites (Table S3). The  
249 most commonly used instruments for this parameter are butanol-based particle counters. Many  
250 FAN sites operate multiple particle counters in tandem which can provide some minimal

251 information on aerosol size distribution because different models have different lower size cuts.  
252 Some sites also operate instruments to measure aerosol size distributions (see Table S3).

253

### 254 **3.2 Infrastructure and Protocols**

255 The FAN is a subset of the WMO Global Atmosphere Watch, and consequently follows the  
256 GAW aerosol guidelines and standard operating procedures (WMO, 2011; 2016). The WMO  
257 World Calibration Center for Aerosol Physics (WCCAP, 2018) organizes instrument training and  
258 evaluation workshops and performs occasional site audits that are designed to ensure consistency  
259 across the GAW network. The role of FAN, in this context, is to provide advice and tools that  
260 make it easier for stations operators to implement the recommended procedures for GAW  
261 stations.

262

263 The FAN standard aerosol inlet configuration (NOAA, 2018b) is slightly anisokinetic (i.e.,  
264 Reynolds number in the range 4500-7000). The resulting turbulent conditions limit losses of  
265 super micrometer particles (Wilcox, 1956). Sampling line sizes, materials, pickoffs, and flow  
266 rates are optimized to promote maximum passing efficiency for particles that are most important  
267 to radiative forcing (i.e., particles with diameters between 0.1 and 10  $\mu\text{m}$ ). Because the focus is  
268 primarily on optically important aerosol, bends in tubing and obstructions upstream of  
269 instruments are minimized to limit particle losses due to impaction. **Passing efficiencies for**  
270 **super-micron particles are 99% and 50% for 1-2 and 7-11  $\mu\text{m}$  aerodynamic diameter particles,**  
271 **respectively. Different inlet designs and/or instruments should be used for aerosol diameters**  
272 **above this size range.** The inlet is not optimized for ultrafine aerosol, however inlet passing  
273 efficiency calculations suggest **a 99% and 50% passing efficiency for 0.1 and 0.002-0.004  $\mu\text{m}$**

274 aerodynamic diameter particles, respectively. Figure S1 in supplemental materials shows the  
275 aerosol inlet passing efficiency for several stations. Some collaborators have designed their own  
276 inlet system (see Table S3). The GAW report 227 (WMO, 2016) includes guidelines for inlet  
277 systems, including criteria and equations used to design them. GAW and FAN offer assistance to  
278 station operators to design inlet systems and calculate losses, but every site is different (e.g.,  
279 surrounding terrain and vegetation, fog frequency) meaning a common design is not practical or  
280 even desirable.

281  
282 The network goal is to make aerosol measurements at low relative humidity ( $RH < 40\%$ ) which  
283 minimizes the confounding effects of aerosol amount and hygroscopicity on the optical  
284 properties, facilitating comparison of aerosol properties among FAN sites. This objective is  
285 consistent with the wider GAW sampling protocol (WMO, 2016). To achieve low RH, two  
286 approaches have been used. The first involves gentle heating (to a maximum of  $40^\circ\text{C}$ ) of the  
287 sample lines and insulation of the sample lines downstream of the heater. Power is only applied  
288 to the heater when the sample humidity is above the desired value. The second approach is to  
289 dilute the air stream with dry, filtered air generated by a compressor system. The dilution  
290 approach is typically used at warm marine sites in the network. The amount of dilution air is  
291 measured and corrections to the measurements are applied automatically during data processing.

292  
293 In order to fully characterize the sampling system, temperature, RH, flow, and pressure are  
294 monitored at several points along the sample line. Monitoring temperature and RH in several  
295 places allows determination of whether sample dewpoint temperature is maintained as the air  
296 moves through the system. Discrepancies in system dewpoint temperature can indicate a leak in

297 the system (or, possibly, a poorly calibrated sensor). Pressure and flow measurements provide  
298 diagnostics to determine whether sample air is flowing through the system as designed.  
299 Additionally, both analog and digital flow and pressure measurements are implemented. The  
300 analog measurements (e.g., rotameters, pressure gauges, etc.) can be assessed at a glance by an  
301 on-site operator. The digital measurements are also available to the on-site operator via the data  
302 acquisition interface, but are primarily intended for someone who is remotely evaluating the  
303 data. Flow diagrams of FAN sites, indicating the locations of sensors and instruments, are  
304 available at (NOAA, 2018c).

305

306 Many FAN sites make aerosol light scattering and absorption coefficient measurements at two  
307 size cuts (aerodynamic particle diameter  $<1$  and  $<10$   $\mu\text{m}$  (PM1 and PM10)). ESRL/GMD has  
308 designed an ‘impactor box’ to smoothly integrate size cut switching into system operations. All  
309 sample air flows through a 10  $\mu\text{m}$  multi-jet Berner impactor (Hillamo and Kauppinen, 1991 and  
310 references therein) prior to being sampled by instruments. On a time base interval ranging from  
311 5 min to 30 min, depending on the site, control software closes an automated ball valve, forcing  
312 the sample flow through a 1  $\mu\text{m}$  Berner impactor. A mass flow controller is used to control flow  
313 through the impactors in order to ensure the desired size cut. The impactor box also contains  
314 solenoid valves that enable the instruments to be bypassed at certain times (e.g., during impactor  
315 cleaning).

316

317 The system requires only minor intervention from on-site technicians. Technician tasks include  
318 nephelometer calibration gas checks (performed with CO<sub>2</sub> and filtered air) to verify instrument  
319 calibration; impactor cleaning; filter changes for the light absorption instruments; and

320 replenishing the operating fluid for number concentration instruments. The frequency of these  
321 tasks depends on the site. Most sites perform nephelometer calibration checks and impactor  
322 servicing on a weekly to monthly basis, while filter changes and operating fluid replenishment  
323 tend to be more frequent. Figure S2 provides an example of nephelometer calibration checks for  
324 FAN sites with at least 5 years of data. Annually, or whenever problems are suspected, FAN  
325 protocols recommend calibration of system sensors (T, P, RH, flow), cleaning of instruments and  
326 sample lines, and overnight filtered air tests on scattering and absorption instruments.

327  
328 It should be noted that there is currently no calibration standard for filter-based absorption  
329 measurements (that is an area of active research, e.g., EMPIRBlackCarbon (2018)) but the flows  
330 for the absorption instruments are calibrated annually. NOAA/GMD does not utilize a  
331 calibration system for particle counters, however, two particle counters are maintained as  
332 reference standards, one of which was tested at the WCCAP **for tying the FAN measurements in**  
333 **with the wider GAW network**. Field CPCs are periodically tested against these lab reference  
334 CPCs. The CPC flows are also checked on a regular basis. Instrument intercomparisons are a  
335 major tool in the aerosol world for ensuring comparable measurements, because some of the  
336 measurements do not have a calibration ‘standards’. Additionally, instrument noise evaluations  
337 are performed annually for scattering, absorption and number concentration instruments; these  
338 evaluations consist of having the instruments measure filtered air for a 12-24 h period.

### 339 **3.3 Software**

340 ESRL/GMD has developed custom software (called CPD3) for acquisition, processing, editing  
341 and archiving of data from aerosol instruments that are used in the FAN. An earlier version of  
342 the ESRL/GMD software (CPD2) is also used in the CATCOS aerosol network (Capacity

343 **Building and Twinning for Climate Observing Systems, PSI (2018)).** The same software suite is  
344 used for both field acquisition computers and offsite data processing and analysis. There is a  
345 simple process to customize a Xubuntu Linux install for running CPD3 in the field. The field  
346 version of CPD3 is used to control instruments and acquire data. Data from CPD3 systems in the  
347 field are typically transmitted to an ftp server operated by NOAA every one to six hours, where  
348 the data are subsequently ingested into a master database that is part of the CPD3 software  
349 system. If desired, the field data can instead be sent to a user-operated server running the CPD3  
350 software system. Scientists and technicians responsible for the data use another copy of CPD3 on  
351 their desktop or laptop computers to review the data for quality and completeness, and flag or  
352 remove contaminated or invalid data. User computers running the CPD3 software regularly  
353 synchronize their local databases with the master database. The synchronization process includes  
354 raw data, editing directives, metadata, and message logs. The CPD3 system supports submission  
355 of both for near real-time (raw data) and annual (QC-reviewed) data to the WMO World Data  
356 Center for Aerosols.

357 NOAA (2018d) further describes software and data flow for the system; all source code for the  
358 CPD3 system is freely available for download (NOAA, 2018d).

359 CPD3 is highly configurable, making it simple to add or remove instruments and change data  
360 logging parameters. A list of instruments that can be logged with CPD3 is available from  
361 NOAA (2018e) . Because all instruments are logged on the same computer using the time server  
362 synched computer timestamp, the timestamp for every instrument is the same. Having all the  
363 instruments and infrastructure tied together enables the system to operate holistically. For  
364 example, if high particle concentrations and/or wind direction indicate local contamination (e.g.,  
365 Sheridan et al., 2016), chemical filters can be automatically bypassed to avoid sampling the



366 contaminated air while other measurements would be flagged. Similarly, during data review, the  
367 ability to inspect multiple data streams simultaneously in a graphical interface can help both with  
368 identifying events and troubleshooting system failures. CPD3 includes a time-stamped message  
369 log enabling the data to be directly related to operator actions and observations both on the  
370 station computer and after the fact during quality control (QC) data inspection and editing.

371  
372 CPD3's graphical interface for data review can be used to look at raw, edited, or averaged station  
373 aerosol data. During the QC process the interface is used by the station scientist to create edit  
374 directives that are applied to the raw data to generate edited data. The raw data files are not  
375 changed in any way. This provides both traceability (the list of edit directives is preserved as  
376 well as the time the edit was generated, identity of the person making the edit and reason for the  
377 edit) and the ability to reprocess the data (e.g., if an improved instrument correction became  
378 available). In order to ensure consistency among different network collaborators, QC editing  
379 strategies are discussed in training and documentation. Details about using the graphical  
380 interface for data QC along with potential system failure modes to look for when editing are  
381 available in the data review documentation (NOAA, 2018f).

382  
383 CPD3 provides tools for editing and applying standard corrections (e.g., standard temperature  
384 and pressure corrections, the truncation correction for the nephelometer (Anderson and Ogren  
385 1998), various schemes for correcting filter-based absorption measurements (e.g., Bond et al.,  
386 1999), etc.), Additionally there are tools for averaging and merging data from different  
387 instruments and outputting the data in various useful formats (raw, averaged, merged, etc). CPD3  
388 is also set up so that near real time, raw and QC'd data in the proper format can be submitted  
389 directly to a database (Tørseth et al., 2012; NILU, 2018) for inclusion in GAW's World Data

390 Centre for Aerosols (WDCA) archive. User-generated metadata from online log entries made by  
391 station personnel are timestamped and available with the data during editing. Instrument-  
392 generated metadata provide reports of system performance, communication issues, warning and  
393 error conditions, and calibration checks, etc. Information on the database tools is available  
394 online (NOAA, 2018g). The end result of the integrated software developed at ESRL/GMD is a  
395 self-consistent data archive standardized across all stations using the software. Final data from  
396 the NOAA/ESRL FAN are available from the WDCA (NILU, 2018) for most stations and from  
397 the PIs in all cases.

398

#### 399 **4. FAN science**

400 While the FAN methodology is useful for a single station, its real strength lies in creating  
401 measurement consistency amongst multiple stations. Science questions that can be addressed  
402 with this data set include:

- 403 • What are the range and variability (on multiple time scales) of aerosol optical properties  
404 observed at FAN sites?
- 405 • How do long-term trends in aerosol properties compare across the globe?

406

407 By combining FAN data with external data sets, additional questions can be explored:

- 408 • Can similarities and differences among sites be related to aerosol types, sources, or  
409 processes?
- 410 • How well do global models and aerosol parameterizations in models capture aerosol  
411 properties across a range of sites?

- 412       • How consistent are the in-situ aerosol properties measured at FAN sites with remote-  
413       sensing measurements from ground- and satellite-based instruments, and how do the  
414       consistencies and inconsistencies inform interpretation of the results from all three  
415       approaches?

416

417 Figure 2 illustrates that the FAN sites cover a wide range of aerosol properties. Aerosol loading  
418 (e.g., scattering and absorption) spans nearly four orders of magnitude. While scattering at the  
419 sites is shown in monotonically increasing order, other aerosol parameters (e.g., single-scattering  
420 albedo and scattering Ångström exponent, see Table 1) vary as a function of the nature of the  
421 particles (e.g., size, composition) rather than aerosol amount. For example, the clean marine  
422 sites (Cape Grim, Australia (CGO), Cape Point, South Africa (CPT), American Samoa (SMO),  
423 Trinidad Head, CA (THD) and Cape San Juan, PR (CPR)) exhibit low scattering Ångström  
424 exponent (SAE) values indicative of large sea salt aerosol, while the low SAE at Mount  
425 Waliguan, China (WLG) can be attributed to large dust particles. Median single-scattering  
426 albedo (SSA) values are around 0.92 at most sites, although the clean marine sites exhibit higher  
427 SSA values due to predominantly white sea salt aerosol. In contrast, UGR exhibits significantly  
428 lower SSA relative to the other sites in the FAN network – the site is strongly impacted by  
429 diesel-based traffic and local biomass burning (Titos et al., 2017). The standardized FAN  
430 sampling and data processing protocols help ensure that the reported differences between stations  
431 are real and not related to operational inconsistencies. Table S1 in the supplemental materials  
432 provides more information about the stations and measurement data depicted in Figure 2. Figure  
433 S3 in supplemental materials shows the same data depicted in Figure 2 in separate sets of panes  
434 with aerosol scattering coefficient ordered by (a) elevation, (b) latitude and (c) longitude.

435

436 While Figure 2 shows annual climatological values for all sites in the network, more detailed  
437 climatologies can be evaluated as well. Figure 3 shows climatological patterns of aerosol light  
438 scattering at Bondville, IL as a function of year, month and day of year. Figure 3a shows that  
439 there has been a decrease in aerosol light scattering at Bondville since the start of measurements  
440 in the mid-1990s and that this decrease appears to have impacted scattering during all months at  
441 the site. This result is consistent with other literature documenting decreases in aerosol loading  
442 over most of the continental U.S. (e.g., Collaud Coen et al., 2013). Although aerosol amounts  
443 have decreased over the last two decades, the general picture of higher scattering during the  
444 summer remains true. Figure 3b depicts how the diurnal cycle varies with time of year. In the  
445 summer, the scattering is high throughout the day, while at other times of year the diurnal cycle  
446 is much more pronounced (similar to the observations of Sherman et al. (2015)). The diurnal  
447 minimum occurs in the early afternoon, most likely due to an increase in boundary layer height.

448

449 Detailed multi-site climatologies, including data from FAN observatories, based on location  
450 (e.g., mountain sites (Andrews et al., 2011); North American sites (e.g., Sherman et al., 2015;  
451 Delene and Ogren, 2002); and Arctic sites (Schmeisser et al., 2018)) have been published. Sites  
452 in the FAN are often members of other networks (e.g., ACTRIS, 2018; IASOA, 2018) and are  
453 included in reports on their climatologies as well (e.g., Uttal et al., 2016; Zanatta et al., 2016;  
454 Pandolfi et al., 2018). Additionally, with multiple sites one can look at the co-variability of  
455 different aerosol properties and start to identify relationships as a function of site and aerosol  
456 type (e.g., Delene and Ogren, 2002; Andrews et al., 2011; Sherman et al., 2015; Schmeisser et  
457 al., 2017). Trend studies have also used data from multiple FAN sites as the focus of their

458 investigation (e.g., Asmi et al., 2013; Collaud Coen et al., 2013; Sherman et al., 2015) to explore  
459 changes in aerosol properties as a function of location. NOAA (2018h) lists FAN data  
460 publications from 2010 to present.

461  
462 An additional advantage of the unified FAN data set is that it can be used to assess and improve  
463 global models. Multiple studies use FAN number concentration data to evaluate various  
464 parameterizations of aerosol nucleation (e.g., Spracklen et al., 2010; Matsui et al., 2013; Mann et  
465 al., 2014; Yu et al., 2014). Skeie et al. (2011) evaluated how well the Oslo CTM2 model  
466 simulated absorbing aerosol in terms of loading and seasonality at multiple FAN stations. There  
467 are several modeling studies using Arctic sites FAN data. For example, Sharma et al. (2013)  
468 explored the sensitivity of absorbing aerosol to wet and dry deposition, while Eckhardt et al.  
469 (2015) used Arctic surface measurements to evaluate simulated model climatologies. Currently,  
470 the FAN data are being utilized to evaluate AEROCOM (Kinne et al., 2006) global model  
471 simulations of surface aerosol scattering and absorption coefficients (Andrews et al., in  
472 preparation, 2018).

473  
474 While the FAN data consistency allows for collective science using data from multiple sites, the  
475 unique locations and interests of scientists involved with each site have also resulted in many  
476 findings. For example, there have been both climatological and transport event-based studies  
477 focused on aerosol types observed at individual sites (e.g., Lim et al., 2012; Hallar et al., 2015;  
478 Sorribas et al., 2015; 2017; Denjean et al., 2016; Rivera et al., 2017; Kassianov et al., 2017).  
479 FAN measurements have been used to provide context for field campaigns (e.g., Brock et al.,  
480 2011; Bravo-Aranda et al., 2015; Denjean et al., 2016), instrument comparisons (e.g., Sharma

481 and Barnes, 2016; Backman et al., 2017; Sinha et al., 2017; Sharma et al., 2017); remote sensing  
482 validation (e.g., Pahlow et al., 2006; Di Pierro et al., 2013; Shinozuka et al., 2015) and many  
483 other scientific efforts.

484

485 Uniting observatories under the umbrella of the Federated Aerosol Network provides the  
486 opportunity to both train and learn from a diverse group of US and international partners. The  
487 federated nature of the network enables scientists to pursue their own interests while  
488 participating in a wider goal, making the network greater than sum of its individual parts. In the  
489 process of increasing understanding of the range and variability in aerosol radiative properties,  
490 the FAN strengthens scientific ties across the globe, fostering collaborations and the exchange of  
491 knowledge. In the FAN's next 25 years, the objective is to maintain current collaborations and  
492 to establish new ones to expand the network, particularly in under-sampled regions. The FAN  
493 will continue to improve measurements, software and protocols in order to be able to address  
494 new questions as they arise.

495

## 496 **5. Conclusions**

497 The FAN is a long-term, cooperative program enabling diverse sites with a wide range of aerosol  
498 types to make measurements that are directly comparable with other network stations. This  
499 facilitates the exploration of science questions at local, regional, and global scales and makes the  
500 network measurements especially useful for global model evaluation. There is a need to expand  
501 such measurements to locations that have large impacts by aerosols but little current  
502 representation in measurement databases, but of course many factors (e.g., funding) will  
503 determine whether this really takes place. The growth and scope of NOAA's collaborative

504 network can be a model for new and existing networks which seek to expand coverage in a  
505 collaborative fashion. For example, in the future, a complementary network comprised of new,  
506 low-cost sensors could be developed or even used to expand the FAN or other networks pending  
507 guidance from GAW's Scientific Advisory Group for Aerosols.

508

### 509 **Acknowledgements**

510 The writing of this manuscript was supported by NOAA Climate Program Office's Atmospheric  
511 Chemistry, Carbon Cycle and Climate (AC4) program. The FAN network would not be possible  
512 without the interest and support of our collaborators and their students and/or technicians who  
513 maintain the stations and instruments, and keep the data flowing from their observatories.

514

515

516 **References**

517 ACTRIS, 2018: Research Infrastructure for the observation of Aerosol, Clouds, and Trace gases.

518 Accessed 21 May 2018, <https://www.actris.eu/>.

519

520 Anderson, T.L., and Coauthors, 2005: An “A-Train” Strategy for Quantifying Direct Climate

521 Forcing by Anthropogenic Aerosols. *Bull. Amer. Meteor. Soc.*, **86**, 1795-

522 1809, <https://doi.org/10.1175/BAMS-86-12-1795>.

523

524 Anderson, T.L. and Ogren, J.A., 1998: Determining aerosol radiative properties using the TSI

525 3563 integrating nephelometer, *Aerosol Sci. Tech.*, **29**, 57-69, doi:10.1080/02786829808965551.

526

527 Andrews, E., and Coauthors, 2018: Comparison of aerosol optical property climatology from in-

528 situ observations and global climate model simulations, in preparation.

529

530 Andrews, E., and Coauthors, 2011: Climatology of aerosol radiative properties in the free

531 troposphere, *Atmos. Res.*, **102**, 365-393, <https://doi.org/10.1016/j.atmosres.2011.08.017>.

532

533 Andrews, E., and Coauthors, 2006: Comparison of methods for deriving aerosol asymmetry

534 parameter, *J. Geophys. Res.*, **111**, doi:10.1029/2004JD005734.

535

536 Andrews, E., Sheridan, P. J., Ogren, J. A., and Ferrare, R., 2004: In situ aerosol profiles over the

537 Southern Great Plains cloud and radiation testbed site: 1. Aerosol optical properties, *J. Geophys.*

538 *Res.*, 109, D06208, doi:10.1029/2003JD004025.



539

540 Asmi, A., and Coauthors, 2013: Aerosol decadal trends – Part 2: In-situ aerosol particle number  
541 concentrations at GAW and ACTRIS stations, *Atmos. Chem. Phys.*, **13**, 895-916,  
542 <https://doi.org/10.5194/acp-13-895-2013>.

543

544 Backman, J. and Coauthors, 2016: On Aethalometer measurement uncertainties and multiple  
545 scattering enhancement in the Arctic, *Atmos. Meas. Tech.*, accepted,  
546 <https://doi.org/10.5194/amt-2016-294>.

547

548 Bodhaine, B. A., 1983: Aerosol measurements at four background sites, *J. Geophys. Res.*, **88**,  
549 10753–10768, doi:10.1029/JC088iC15p10753.

550

551 Bolin, B. and Charlson, R.J., 1976: On the role of the tropospheric sulfur cycle in the shortwave  
552 radiative climate of the Earth, *Ambio*, **3**, 47-54.

553

554 Bond, T. C., Anderson, T. L., and Campbell, D., 1999: Calibration and intercomparison of filter-  
555 based measurements of visible light absorption by aerosols, *Aerosol Sci. Technol.*, **30**, 582–600,  
556 doi:10.1080/027868299304435.

557

558 Bravo-Aranda, J.A. and Coauthors, 2015: Study of mineral dust entrainment in the planetary  
559 boundary layer by lidar depolarisation technique, *Tellus B*, **67**, 26180, doi:  
560 10.3402/tellusb.v67.26180.

561

562 Brock, C.A. and Coauthors, 2011: Characteristics, sources, and transport of aerosols measured in  
563 spring 2008 during the aerosol, radiation, and cloud processes affecting Arctic Climate  
564 (ARCPAC) Project, *Atmos. Chem. Phys.*, **11**, 2423-2453,  
565 <https://doi.org/10.5194/acp-11-2423-2011>.  
566

567 Charlson, R.J., Langner, J., Rodhe, H., Leovy, C.B., and Warren, S.G., 1991: Perturbation of the  
568 northern hemisphere radiative balance by backscattering from anthropogenic sulfate aerosols,  
569 *Tellus*, **43AB**, 152-163, doi:10.1034/j.1600-0870.1991.00013.x.  
570

571 Collaud Coen, M., and Coauthors, 2013: Aerosol decadal trends – Part 1: In-situ optical  
572 measurements at GAW and IMPROVE stations, *Atmos. Chem. Phys.*, **13**, 869-894,  
573 <https://doi.org/10.5194/acp-13-869-2013>.  
574

575 Collins., 2018: Definition of 'federated'. Accessed 21 May 2018,  
576 <https://www.collinsdictionary.com/us/dictionary/english/federated>  
577

578 Delene, D. J. and Ogren, J. A., 2002: Variability of aerosol optical properties at four North  
579 American surface monitoring sites, *J. Atmos. Sci.*, **59**, 1135–1150, doi:10.1175/1520-  
580 0469(2002)059<1135:VOAOPA>2.0.CO;2.  
581

582 Denjean, C. and Coauthors, 2016: Size distribution and optical properties of African mineral dust  
583 after intercontinental transport, *J. Geophys. Res.*, **121**, 7117-7138, doi:10.1002/2016JD024783.  
584

585 Di Pierro, M., Jaegle, L., Eloranta, E.W., Sharma, S., 2013: Spatial and seasonal distribution of  
586 Arctic aerosols observed by the CALIOP satellite instrument (2006–2012), *Atmos. Chem. Phys.*,  
587 **13**, 13, 7075-7095, <https://doi.org/10.5194/acp-13-7075-2013>.  
588

589 Eckhardt, S. and Coauthors, 2015: Current model capabilities for simulating black carbon and  
590 sulfate concentrations in the Arctic atmosphere: a multi-model evaluation using a comprehensive  
591 measurement data set, *Atmos. Chem, Phys.*, **15**, 9413–9433, doi:10.5194/acp-15-9413-2015.  
592

593 EMPIRBlackCarbon, 2018: Black Carbon Metrology for light absorption by atmospheric  
594 aerosols. Accessed 21 May 2018, <http://www.empirblackcarbon.com>.  
595

596 Hallar, A.G., Petersen, R., Andrews, E., Michalsky, J., McCubbin, I., Ogren, J.A., 2015:  
597 Contributions of dust and biomass-burning to aerosols at a Colorado mountain-top site, *Atmos.*  
598 *Chem. Phys.*, **15**, 13665-13679, <https://doi.org/10.5194/acp-15-13665-2015>.  
599

600 Hillamo, R.E. and Kauppinen, E.I, 1991: On the performance of the Berner low pressure  
601 impactor, *Aerosol Sci. Technol.*, **14**, 33-47, doi: 10.1080/02786829108959469.  
602

603 Holben, B.N. and Coauthors, 1998: AERONET - A federated instrument network and data  
604 archive for aerosol characterization. *Remote Sensing of Environment*, **66**, 1-16,  
605 [https://doi.org/10.1016/S0034-4257\(98\)00031-5](https://doi.org/10.1016/S0034-4257(98)00031-5).  
606

607 IASOA, 2018: International Arctic Systems for Observing the Atmosphere. Accessed 21 May  
608 2018, <https://www.esrl.noaa.gov/psd/iasoa/>.  
609

610 IPCC, 2013: Climate Change 2013: The Physical Science Basis. Contribution of Working  
611 Group I to the Fifth Assessment Report of the Intergovernmental Panel on Climate Change,  
612 [Stocker, T.F., D. Qin, G.-K. Plattner, M. Tignor, S.K. Allen, J. Boschung, A. Nauels, Y. Xia, V.  
613 Bex and P.M. Midgley (eds.)]. Cambridge University Press, Cambridge, United Kingdom and  
614 New York, NY, USA, 1535 pp, doi:10.1017/CBO9781107415324.  
615

616 Kahn, R.A. and Coauthors, 2004: Aerosol data sources and their roles within PARAGON, *Bull.*  
617 *Amer. Meteor. Soc.*, **85**, 1155-1122, <https://doi.org/10.1175/BAMS-85-10-1511>.  
618

619 Kahn, R.A. and Coauthors, 2017: SAM-CAAM: A Concept for Acquiring Systematic Aircraft  
620 Measurements to Characterize Aerosol Air Masses, *Bull. Amer. Meteor. Soc.*, **98**, 2215-2228,  
621 <https://doi.org/10.1175/BAMS-D-16-0003.1>.  
622

623 Kassianov, E. and Coauthors, 2017: Large Contribution of Coarse Mode to Aerosol  
624 Microphysical and Optical Properties: Evidence from Ground-Based Observations of a  
625 Transpacific Dust Outbreak at a High-Elevation North American Site, *J. Atmos. Sci.*, **74**, 1431-  
626 1443, <https://doi.org/10.1175/JAS-D-16-0256.1>.  
627

628 Kinne, S., and Coauthors, 2006: An AeroCom initial assessment – optical properties in aerosol  
629 component modules of global models, *Atmos. Chem. Phys.*, **6**, 1815–1834, doi:10.5194/acp-6-  
630 1815-2006.

631

632 Kulmala M., and Coauthors, 2011: General overview: European Integrated project on Aerosol  
633 Cloud Climate and Air Quality interactions (EUCAARI) – integrating aerosol research from  
634 nano to global scales, *Atmos. Chem. Phys.*, **11**, 13061–13143, [https://doi.org/10.5194/acp-11-](https://doi.org/10.5194/acp-11-13061-2011)  
635 13061-2011.

636

637 Laj, P., and Coauthors, 2009: Measuring atmospheric composition change, *Atmos. Environ.*, **43**,  
638 5351-5414, doi:10.1016/j.atmosenv.2009.08.020.

639

640 Lim, S., Lee, M., Lee, G., Kim, S., Kang, K., 2012: Ionic and carbonaceous compositions of  
641 PM10, PM2.5 and PM1.0 at Gosan ABC Superstation and their ratios as source signature,"  
642 *Atmos. Chem. Phys.*, **12**, 2007-2024, <https://doi.org/10.5194/acp-12-2007-2012>.

643

644 Lund Myhre, C. and Baltensperger, U., 2012: Recommendations for a Composite Surface-Based  
645 Aerosol Network, WMO/GAW Report 207, World Meteorological Organization, Geneva,  
646 [http://library.wmo.int/pmb\\_ged/gaw\\_207.pdf](http://library.wmo.int/pmb_ged/gaw_207.pdf).

647

648 Mann, G.W. and Coauthors, 2014: Intercomparison and evaluation of global aerosol  
649 microphysical properties among AeroCom models of a range of complexity, *Atmos. Chem.*  
650 *Phys.*, **14**, 4679–4713, doi:10.5194/acp-14-4679-2014.

651

652 Matsui, H. and Coauthors, 2013: Spatial and temporal variations of new particle formation in  
653 East Asia using an NPF-explicit WRF-chem model: North-south contrast in new particle  
654 formation frequency, *J. Geophys. Res.*, **118**, 11647–11663, doi:10.1002/jgrd.50821.

655

656 Mueller, T. and Coauthors, 2011a: Characterization and intercomparison of aerosol absorption  
657 photometers: result of two intercomparison workshops, *Atmos. Meas. Tech.*, 4, 245-268,  
658 doi:10.5194/amt-4-245-2011.

659

660 Mueller, T., Laborde, M., Kassell, G., and Wiedensohler, A., 2011b: Design and performance of  
661 a three-wavelength LED-based total scatter and backscatter integrating nephelometer, *Atmos.*  
662 *Meas. Tech.*, 4, 1291-1303, doi:10.5194/amt-4-1291-2011.

663

664 NILU, 2018: EMEP: Hosting the GAW WDCA, Accessed 21 May 2018, <http://ebas.nilu.no/>.

665

666 NOAA, 2018a: ESRL/GMD Aerosol Measurements. Accessed 21 May 2018,  
667 <https://www.esrl.noaa.gov/gmd/aero/instrumentation/instrum.html>.

668

669 NOAA, 2018b: Aerosol System Inlet. Accessed 21 May 2018,  
670 [https://www.esrl.noaa.gov/gmd/aero/instrumentation/inlet\\_system.html](https://www.esrl.noaa.gov/gmd/aero/instrumentation/inlet_system.html).

671

672 NOAA, 2018c: Station flow diagrams. Accessed 21 May 2018,  
673 <ftp://aftp.cmdl.noaa.gov/aerosol/doc/drawings/stn/>.

674 NOAA, 2018d: Aerosols Software. Accessed 21 May 2018,  
675 <https://www.esrl.noaa.gov/gmd/aero/sw.html>  
676  
677 NOAA, 2018e: CPD3 loggable instruments. Accessed 21 May 2018,  
678 [https://www.esrl.noaa.gov/gmd/instrumentation/cpd\\_inst.html](https://www.esrl.noaa.gov/gmd/instrumentation/cpd_inst.html)  
679  
680 NOAA, 2018f: CPD3. Accessed 21 May 2018,  
681 [ftp://aftp.cmdl.noaa.gov/aerosol/etc/cpd3\\_doc/Using\\_CPX3.pdf](ftp://aftp.cmdl.noaa.gov/aerosol/etc/cpd3_doc/Using_CPX3.pdf)  
682  
683 NOAA, 2018g: CPD3. Accessed 21 May 2018,  
684 <https://www.esrl.noaa.gov/gmd/webdata/aero/net/cpd3/doc/>  
685  
686 NOAA, 2018h: Network publications. Accessed 21 May 2018,  
687 <ftp://aftp.cmdl.noaa.gov/aerosol/doc/newsletter/publications.html>.  
688  
689 Ogren, J.A., 1995: A systematic approach to in-situ observation of aerosol properties, In:  
690 *Aerosol Forcing of Climate*, eds. R. Charlson and J. Heintzenberg, John Wiley & Sons, Ltd.,  
691 215-226.  
692  
693 Ogren, J.A., Wendell, J., Andrews, E., and Sheridan, P., 2017: Continuous light absorption  
694 photometer for long-term studies, *Atmos. Meas. Tech.*, **10**, 4805-4818,  
695 <https://doi.org/10.5194/amt-10-4805-2017>.  
696

697 Pahlow, M. and Coauthors, 2006: Comparison between lidar and nephelometer measurements of  
698 aerosol hygroscopicity at the Southern Great Plains Atmospheric Radiation Measurement site, *J.*  
699 *Geophys. Res.*, **111**, doi:10.1029/2004JD005646.

700

701 Pandolfi, M. and Coauthors, 2018: A European aerosol phenomenology-6: Scattering properties  
702 of atmospheric aerosol particles from 28 ACTRIS sites, *Atmos. Chem. Phys.* accepted for  
703 publication.

704

705 Perry, K.D., Cahill, T.A., Schnell, R.C., and Harris, J.M., 1999: Long-range transport of  
706 anthropogenic aerosols to the National Oceanic and Atmospheric Administration baseline station  
707 at Mauna Loa Observatory, Hawaii, *J. Geophys. Res.*, **104**, 18521-18533,  
708 doi:10.1029/1998JD100083.

709

710 PSI, 2018: CATCOS Aerosol Measurements. Accessed 21 May 2018,  
711 <https://www.psi.ch/catcos/>.

712

713 Rivera, H., Ogren, J.A., Andrews, E., Mayol-Bracero, O.L., 2017: Variations in the  
714 physicochemical and optical properties of natural aerosols in Puerto Rico – Implications for  
715 climate, *Atmos. Chem. Phys. Disc.*, in review, <https://doi.org/10.5194/acp-2017-703>.

716

717 Schmeisser, L., and Coauthors, 2017: Classifying aerosol type using in-situ surface spectral  
718 aerosol optical properties, *Atmos. Chem. Phys.*, **17**, 12097-12120, [https://doi.org/10.5194/acp-17-](https://doi.org/10.5194/acp-17-12097-2017)  
719 [12097-2017](https://doi.org/10.5194/acp-17-12097-2017).



720

721 Schmeisser, L., and Coauthors, 2018: Seasonality of aerosol optical properties in the Arctic,  
722 *Atmos. Chem. Phys. Disc.*, in review, <https://www.atmos-chem-phys-discuss.net/acp-2017-1117..>

723

724 Sharma, N.C.P., Barnes, J.E., 2016: Boundary layer characteristics over a high altitude station,  
725 Mauna Loa Observatory, *Aerosol Air Qual. Res.*, **16**, 729-737, doi:10.4209/aaqr.2015.05.0347.

726

727 Sharma, S., and Coauthors, 2017: An evaluation of three methods for measuring black carbon at  
728 Alert, Canada, *Atmos. Chem. Phys. Discuss.*, **17**, <https://doi.org/10.5194/acp-2017-339>, in  
729 review.

730

731 Sharma, S., Ishizawa, M, Chan, D., Lavoué, D., Andrews, E., Eleftheriadis, K and  
732 Maksyutov, S., 2013: 16-year simulation of Arctic black carbon: transport, source contribution,  
733 and sensitivity analysis on deposition, *J. Geophys. Res.*, **118**, doi:10.1029/2012JD017774.

734

735 Sheridan, P.J., Delene, D.J., and Ogren, J.A., 2001: Four years of continuous surface aerosol  
736 measurements from the Department of Energy's Atmospheric Radiation Measurement Program  
737 Southern Great Plains Cloud and Radiation Testbed site, *J. Geophys. Res.* **106**, 20735-20747,  
738 doi:10.1029/2001JD000785.

739

740 Sheridan, P.J., Andrews, E., Ogren, J.A., Tackett, J., Winker, D.M., 2012: Vertical profiles of  
741 aerosol optical properties over central Illinois and comparison with surface and satellite  
742 measurements," *Atmos. Chem. Phys.*, **12**, 11695-11721, doi: 10.5194/acp-12-11695-2012.

743

744 Sheridan, P.J., Andrews, E., Schmeisser, L., Vasel, B., and Ogren, J.A., 2016: Aerosol  
745 Measurements at South Pole: Climatology and Impact of Local Contamination, *AAQR*, **16**, 855-  
746 872, doi:10.4209/aaqr.2015.05.0358.

747

748 Sherman, J.P., Sheridan, P.J., Ogren, J.A., Andrews, E., Hageman, D.C., Schmeisser, L.,  
749 Jefferson, A., and Sharma, S., 2015: A multi-year study of lower tropospheric aerosol variability  
750 and systematic relationships from four North American regions, *Atmos. Chem. Phys.*, **15**, 12487-  
751 12517, <https://doi.org/10.5194/acp-15-12487-2015>.

752

753 Shinozuka, Y., and Coauthors, 2015: The relationship between cloud condensation nuclei (CCN)  
754 concentration and light extinction of dried particles: indications of underlying aerosol processes  
755 and implications for satellite-based CCN estimates, *Atmos. Chem. Phys.*, **15**, 7585-7604,  
756 <https://doi.org/10.5194/acp-15-7585-2015>.

757

758 Sinha, P.R. and Coauthors, 2017: Evaluation of ground-based black carbon measurements by  
759 filter-based photometers at two Arctic sites, *J. Geophys. Res.*, **122**, 3544-3572,  
760 doi:10.1002/2016JD025843.

761

762 Skeie, R.B, Berntsen, T., Myhre, G., Pedersen, J.A., Strom, J., Gerland, S., and Ogren, J.A.,  
763 2011: Black carbon in the atmosphere and snow, from pre-industrial times until present, *Atmos.*  
764 *Chem. Phys.*, **11**, 6809-6836, <https://doi.org/10.5194/acp-11-6809-2011>.

765

766 Sorribas, M., Andrews, E., Adame, J.A., Yela, M., 2017: An anomalous African dust event and  
767 its impact on aerosol radiative forcing on the Southwest Atlantic coast of Europe in February  
768 2016, *Sci. Tot. Environ.*, **583**, 269-279, <https://doi.org/10.1016/j.scitotenv.2017.01.064>.  
769

770 Sorribas, M., Ogren, J.A., Olmo, F.J., Quirantes, A., Fraile, R., Gil-Ojeda, M., Alados-  
771 Arboledas, L., 2015: Assessment of African desert dust episodes over the southwest Spain at sea  
772 level using in situ aerosol optical and microphysical properties, *Tellus B*, **67**, doi:  
773 <https://doi.org/10.3402/tellusb.v67.27482>.  
774

775 Spracklen, D. V., and Coauthors, 2010: Explaining global surface aerosol number concentrations  
776 in terms of primary emissions and particle formation, *Atmos. Chem. Phys.*, **10**, 4775-4793,  
777 <https://doi.org/10.5194/acp-11-10661-2011>.  
778

779 Stone, R.S., Anderson, G.P., Andrews, E., Dutton, E.G., and Shettle, E.P., 2007: Incursions and  
780 radiative impact of Asian dust in northern Alaska, *Geophys. Res. Lett.*, **34**,  
781 doi:10.1029/2007GL029878 .  
782

783 Titos, G. and Coauthors, 2017: Spatial and temporal variability of carbonaceous aerosols:  
784 Assessing the impact of biomass burning in the urban environment, *Sci. Tot. Environ.*, **578**, 613-  
785 625, doi:10.1016/j.scitotenv.2016.11.007.  
786

787 Tørseth and Coauthors, 2012: Introduction to the European Monitoring and Evaluation  
788 Programme (EMEP) and observed atmospheric composition change during 1972-2009, *Atmos.*  
789 *Chem. Phys.*, **12**, 5447-5481, doi:10.5194/acp-12-5447-2012.

790

791 Uttal T., and Coauthors, 2016: International Arctic Systems for Observing the Atmosphere: An  
792 International Polar Year Legacy Consortium, *Bull. Amer. Meteor. Soc.*, **97**, 1033-1056,  
793 <https://doi.org/10.1175/BAMS-D-14-00145.1>.

794

795 Wang, R., and Coauthors, 2018: Representativeness error in the ground-level observation  
796 networks for black carbon radiation absorption, *Geophys. Res. Lett.*, doi:10.1002/2017GL076817.

797

798 WCCAP, 2018: World Calibration Centre for Aerosol Physics, Accessed 21 May 2018,  
799 <http://www.wmo-gaw-wcc-aerosol-physics.org>.

800

801

802 Wiedensohler, A., and Coauthors, 2012: Mobility particle size spectrometers: harmonization of  
803 technical standards and data structure to facilitate high quality long-term observations of  
804 atmospheric particle number size distributions, *Atmos. Meas. Tech.*, **5**, 657-685,  
805 doi:10.5194/amt-5-657-2012.

806

807 Wilcox, J.D., 1956: Isokinetic Flow and Sampling, *J. Air Poll. Contr. Assoc.*, **5**, 226-245, doi:  
808 10.1080/00966665.1956.10467715

809

810 WMO, 2011: WMO/GAW Standard Operating Procedures for In-situ Measurements of Aerosol  
811 Mass Concentration, Light Scattering and Light Absorption, GAW Report No. 200, World  
812 Meteorological Organization, Geneva, [http://library.wmo.int/pmb\\_ged/gaw\\_200.pdf](http://library.wmo.int/pmb_ged/gaw_200.pdf).

813

814 WMO, 2016: WMO/GAW Aerosol Measurement Procedures, Guidelines, and  
815 Recommendations, GAW Report No. 227, World Meteorological Organization, Geneva,  
816 [https://library.wmo.int/opac/doc\\_num.php?explnum\\_id=3073](https://library.wmo.int/opac/doc_num.php?explnum_id=3073).

817

818 Yu, F. and Hallar, A.G., 2014: Difference in particle formation at a mountaintop location during  
819 spring and summer: implications for the role of sulfuric acid and organics in nucleation, *J.*  
820 *Geophys. Res.*, **119**, 12246-12255, doi:10.1002/2014JD022136.

821

822 Zanatta, M. and Coauthors, 2016: A European aerosol phenomenology-5: Climatology of black  
823 carbon optical properties at 9 regional background sites across Europe, *Atmos. Environ.*, **145**,  
824 346-364, <http://dx.doi.org/10.1016/j.atmosenv.2016.09.035>.

825

826 **Table 1. Description of aerosol parameters mentioned in text**

<b>Aerosol Parameter (symbol)</b>	<b>Description of parameter and measurement instrument or equation for calculating</b>
<b>Aerosol Light Scattering (<math>\sigma_{sp}</math>)</b>	Indicator of aerosol amount and related optical effects. Measured in the FAN with an integrating nephelometer.
<b>Aerosol Light Absorption (<math>\sigma_{ap}</math>)</b>	Indicator of particle darkness; related to black carbon (BC). Measured in the FAN with a filter-based absorption photometer.
<b>Aerosol Number Concentration (N)</b>	Indicator of local contamination; precursor of cloud condensation nuclei. Measured in the FAN with a condensation particle counter.
<b>Scattering Ångström exponent (SAE)</b>	SAE describes the wavelength-dependence of scattered light. When scattering is dominated by sub-micrometer particles the SAE values are typically around 2, while SAE values closer to 0 occur when the scattering is dominated by particles larger than a few micrometers in diameter. $SAE = -\log[\sigma_{sp}(\lambda_1)/\sigma_{sp}(\lambda_2)]/\log(\lambda_2/\lambda_1)$
<b>Single-scattering albedo (SSA)</b>	SSA describes the relative contributions of scattering and absorption to the total light extinction. Purely scattering aerosols (e.g., sulfuric acid) have SSA values of 1, while very strong absorbers (e.g., elemental carbon) have SSA values around 0.3. $SSA = \sigma_{sp}/(\sigma_{sp} + \sigma_{ap})$

828 **Figure Captions**

829

830 Figure 1. Map of current and former long-term sites in FAN network superimposed on a  
831 nighttime lights image (Credit: NASA Earth Observatory/NOAA NGDC). Former sites RSL,  
832 SGP and WSA were FAN collaborations, while THD and SMO were solely NOAA  
833 observations.

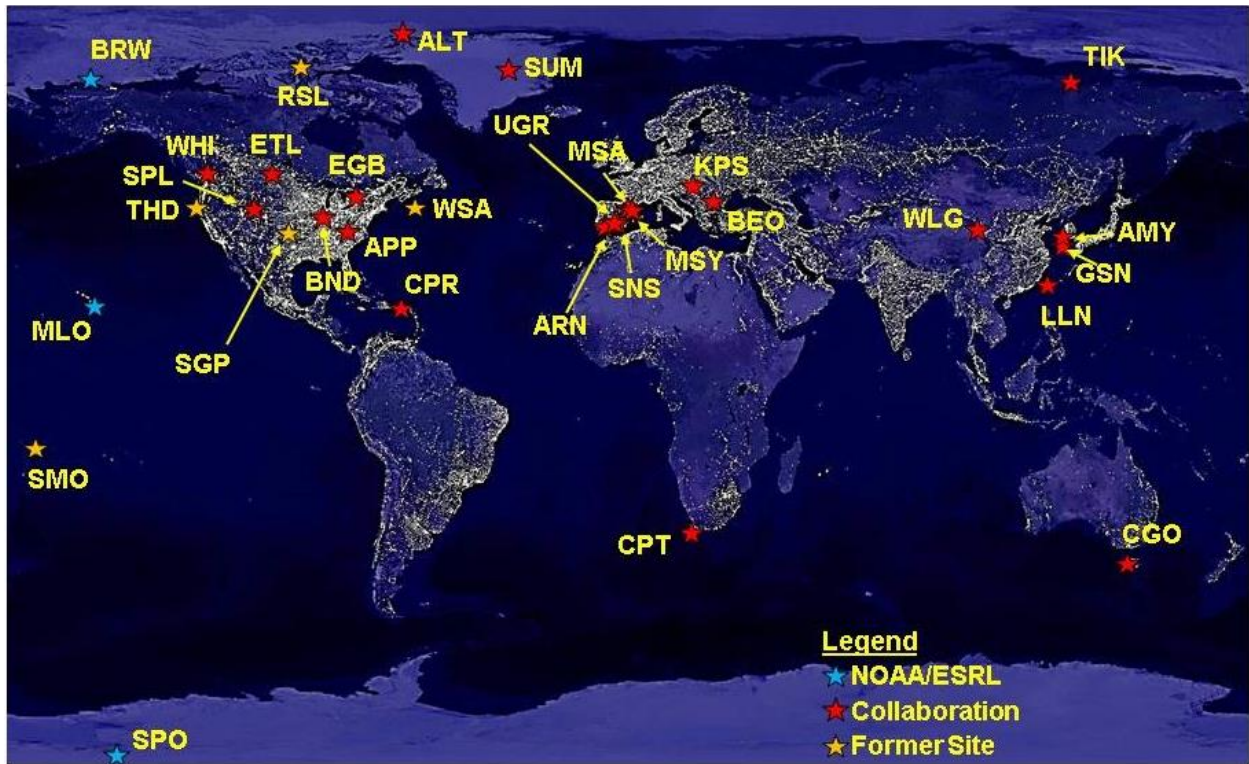
834

835 Figure 2. Annual aerosol climatology for long-term sites in network. Stations are ordered by  
836 increasing scattering coefficient. (a) scattering coefficient; (b) absorption coefficient; (c)  
837 scattering Ångström exponent (d) single-scattering albedo. Scattering and absorption have units  
838 of  $Mm^{-1}$ , scattering Ångström exponent and single-scattering albedo are unitless. Values are  
839 reported at 550 nm, scattering Ångström exponent is calculated for the blue/green wavelength  
840 pair. Whiskers represent 5<sup>th</sup> and 95<sup>th</sup> percentiles, edges of box are 25<sup>th</sup> and 75<sup>th</sup> percentiles and  
841 midpoint line in box is median value of annual climatology. Blue indicates NOAA observatories,  
842 red indicates collaborator sites. Some sites are not shown due little available data (e.g., less than  
843 a year of data available or data not yet being QC'd).

844

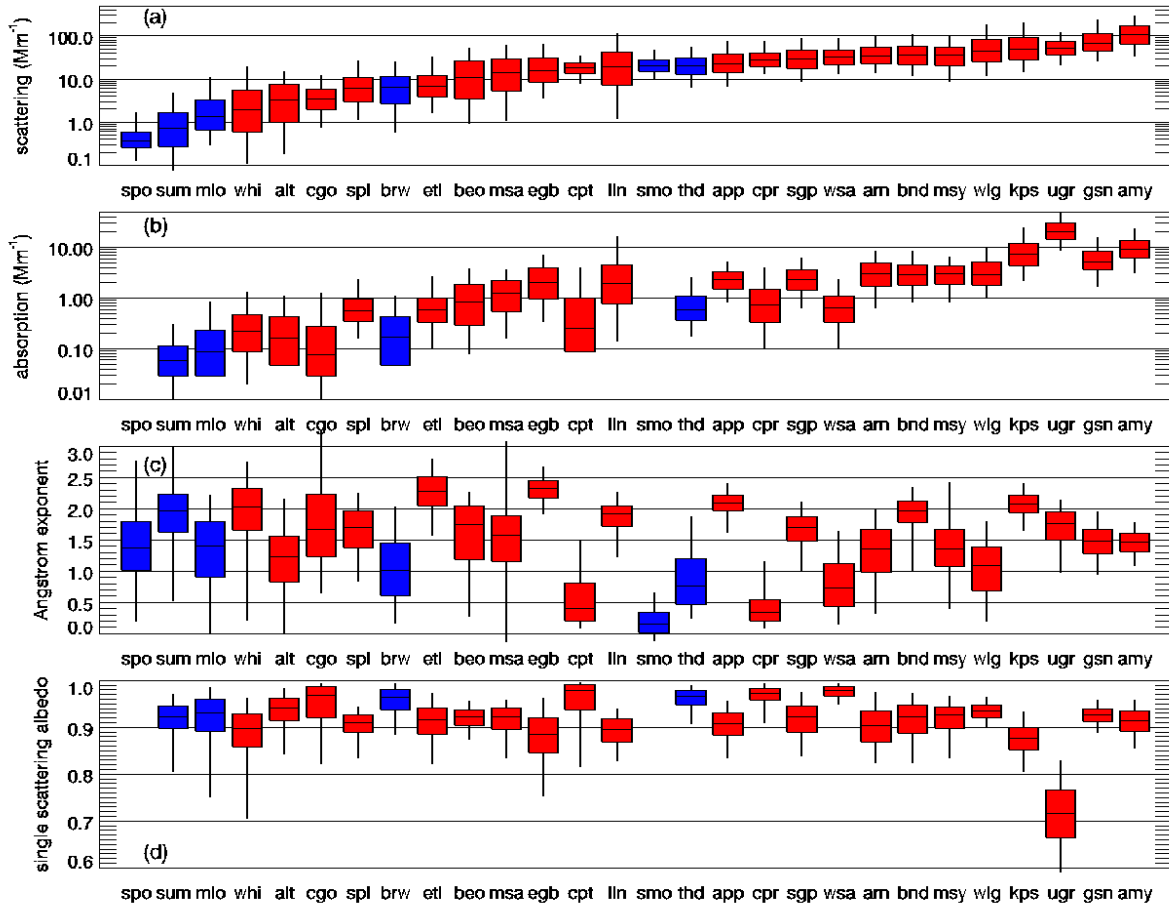
845 Figure 3. Long-term climatology of aerosol light scattering (at 550 nm) in units of  $Mm^{-1}$  at  
846 Bondville. (a) monthly variability as function of year; (b) diurnal variability as function of month  
847 (thick black horizontal line indicates local noon). Both plots are based on data obtained from  
848 1995 through 2016.

849



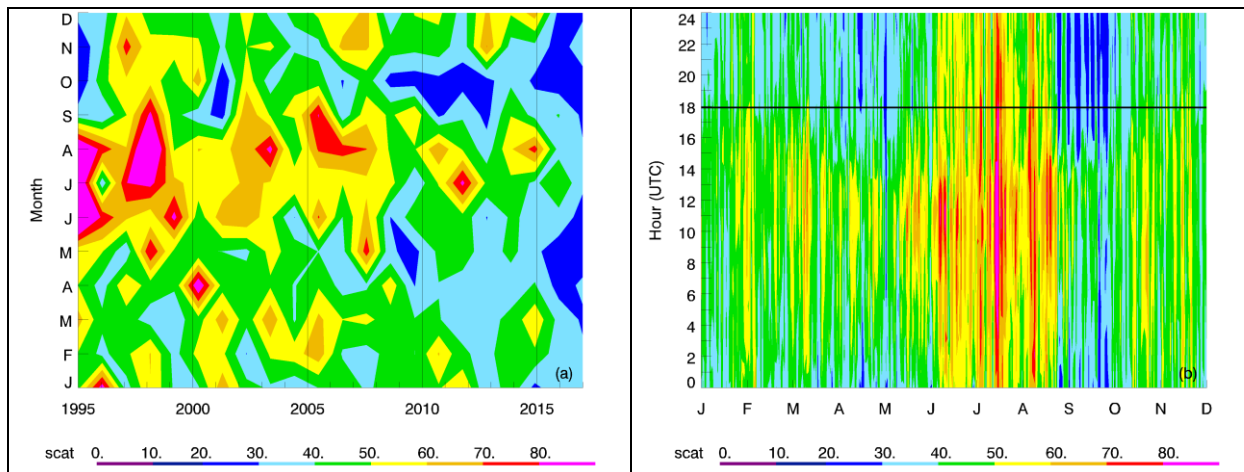
850  
 851 Figure 1. Map of current and former long-term sites in FAN network superimposed on a  
 852 nighttime lights image (Credit: NASA Earth Observatory/NOAA NGDC). Former sites RSL,  
 853 SGP and WSA were FAN collaborations, while THD and SMO were solely NOAA  
 854 observations.





855  
 856 Figure 2. Annual aerosol climatology for long-term sites in network. Stations are ordered by  
 857 increasing scattering coefficient. (a) scattering coefficient; (b) absorption coefficient; (c)  
 858 scattering Ångström exponent (d) single-scattering albedo. Scattering and absorption have units  
 859 of  $\text{Mm}^{-1}$ , scattering Ångström exponent and single-scattering albedo are unitless. Values are  
 860 calculated from daily averages reported at (or adjusted to) 550 nm, scattering Ångström exponent  
 861 is calculated for the blue/green wavelength pair. Whiskers represent 5<sup>th</sup> and 95<sup>th</sup> percentiles,  
 862 edges of box are 25<sup>th</sup> and 75<sup>th</sup> percentiles and midpoint line in box is median value of annual  
 863 climatology. Blue indicates NOAA observatories, red indicates collaborator sites. Some sites are  
 864 not shown due to little available data (e.g., less than a year of data available or data not yet being  
 865 QC'd).

866



867  
 868 Figure 3. Long-term climatology of aerosol light scattering (at 550 nm) in units of  $\text{Mm}^{-1}$  at  
 869 Bondville. (a) monthly variability as function of year; (b) diurnal variability as function of month  
 870 (thick black horizontal line indicates local noon). Both plots are based on data obtained from  
 871 1995 through 2016.